Revised identification of the G-levels in gold doped Si by Laplace deep level transient spectroscopy

K. Gwozdz,[1] Vl. Kolkovsky,[2,a)] V. Kolkovsky,[2] and J. Weber[2]
[1]*Department of Quantum Technologies, Faculty of Fundamental Problems of Technology, Wroclaw University of Science and Technology, Wybrzeze Wyspianskiego 27, 50-370 Wroclaw, Poland*
[2]*Technische Universität Dresden, 01062 Dresden, Germany*

(Received 19 April 2018; accepted 13 June 2018; published online 2 July 2018)

In this study, we re-examine the electronic levels G1-G4 of gold-hydrogen complexes in Si by Laplace deep level transient spectroscopy. In Au doped n- and p-type Si, we analyse the depth profiles of the levels after wet-chemical etching, study their annealing behaviour and detect changes of their emission rates in the electrical field. We give evidence that G1, G3, and G2 are the double acceptor, acceptor, and donor level of the Au complex with one hydrogen atom, whereas G4 belongs to the Au complex with two hydrogen atoms and is probably an acceptor level. *Published by AIP Publishing*. https://doi.org/10.1063/1.5036807

I. INTRODUCTION

The electrical and optical properties of the efficient gold recombination centre in Si have been extensively studied during the last decades. In several studies, a single acceptor (E_C −0.56 eV) and a single donor (E_V +0.35 eV) level of the same substitutional Au (Au_S) impurity were identified.[1,2] Based on deep level transient spectroscopy (DLTS) measurements Lang and co-workers reported dissimilar Au donor and acceptor concentrations in their diodes and questioned the common origin of both levels.[3] However, a proper calculation of the occupation of the neutral state performed in photocapacitance or DLTS measurements showed that these two levels belonged to the same defect.[4,5] A similar conclusion was drawn from the analysis of implanted radioactive Hg nuclei, which decay into unstable Au isotopes on substitutional sites.[6] The controversy was ended, when Watkins and co-workers measured the Zeeman splitting of the optical transitions from the donor and acceptor ground states to their respective excited effective mass like states.[7] The neutral state of the donor and acceptor transitions exhibited an identical g-factor, which confirmed the attribution of the two levels to the same Au center.

Hydrogenation of the Au_S donor and acceptor level was first studied in samples treated in an H-plasma or by electrolytic hydrogen charging in acids.[8,9] Partial and even complete neutralization of the Au_S states was observed depending on the temperatures of hydrogen treatment (200–350 °C). Electrically active levels of AuH complexes were first detected by Sveinbjörnson and Engström after wet chemical etching (WCE) of the samples at room temperatures.[10,11] The authors attributed three defect levels G1 ($E_C - 0.19$ eV), G4 (midgap), and G2 ($E_V + 0.21$ eV) to the same AuH complex, which was tentatively proposed as a single hydrogen atom bound to substitutional Au (AuH_1). The attribution of G1 and G4 to different charge states of the same defect was based on their comparable (but not identical) depth profiles and the similar annealing behaviour of these defects. In addition, a transformation of the electrically active AuH complex with additional hydrogen into a passive defect was detected. Besides G1, G2, and G4 another level G3 ($E_C - 0.47$ eV) was also reported in Refs. 10 and 11. Its annealing behaviour was different from that assigned to the AuH_1 complex and G3 was attributed to a AuH-related complex.

These results were supported by a combination of DLTS and minority carrier transient spectroscopy (MCTS) measurements on Au doped *n*-type Si.[12] Based on the measured minority and majority carrier capture cross sections, the levels were assigned to single donor (G2), single acceptor (G4), and double acceptor (G1) charge states.

The electrical levels of G4 and $Au_S(-/0)$ have almost identical electrical properties and they cannot be resolved properly by the conventional DLTS technique. Therefore, the determination of the concentration profile of G4 in Ref. 11 was performed under the assumption that this defect should be dominant close to the hydrogenated surface. Zamouche[13] reported a different annealing behaviour of G1 and G4 in *n*-type Si, and this was not consistent with the assignment of these peaks to different charge states of the same defect. A Laplace DLTS (LDLTS) study finally separated the G4 from the $Au_S(-/0)$ level and allowed a direct measurement of the activation energy and the capture cross section of G4.[14] Parakhonskii *et al.*[15] observed a DLTS peak at about 200 K after a dc H-plasma treatment in *n*-type Si. This level was assigned to the AuH_3 complex, which, however, has never been observed in other studies.

Several hydrogen-vibrational modes were detected in Au doped Si after in diffusion of hydrogen/deuterium at high temperatures.[16] Two centres with one and two equivalent hydrogen atoms bound to Au (AuH_1 and AuH_2) are responsible for the detected stretching modes. From the intensity changes of the AuH_1 vibrational modes with the Fermi level, three charge states with a level above the Au_S acceptor level and a second level located in the lower half of the band gap were identified.

The presence of a AuH_2 complex in hydrogenated Si was also reported by electron paramagnetic resonance

a)kolkov@ifpan.edu.pl

measurements.[17] The symmetry of this complex was established as triclinic, and a microscopic model was presented with an Au atom at the substitutional site and two hydrogen atoms at the interstitial sites which are anti-bonding to the silicon nearest neighbours. Unfortunately, no energy position of this level in the band gap of Si was given.

In this study, we analyse the AuH-related levels G1-G4 in hydrogenated Au-doped *n*- and *p*-type Si samples by the LDLTS technique.[18] We determine the depth profiles of all levels and study their annealing behaviour. The charge state of the defect levels cannot be measured directly by the DLTS technique, although from the magnitude of the capture cross section a donor or an acceptor behaviour could be deduced. We determine changes of the emission rates as a function of the electrical field in the space charge region to gather additional information about their charge states. Our results give a direct confirmation that the G1 and G2 levels belong to the same Au complex with only one hydrogen atom (AuH_1). In contrast to most of the previous studies, we clarify that G4 belongs to another charge state of AuH_1 and G3 to an Au complex with two hydrogen atoms (AuH_2). We associate G1, G3, and G2 with the double acceptor, acceptor, and donor levels of AuH_1. Level G4 is probably the single acceptor state of AuH_2.

II. EXPERIMENTAL

We used in this study Float-zone Si samples with P or B as shallow dopants in the concentration range $5 \times 10^{14}\,cm^{-3}$–$3 \times 10^{15}\,cm^{-3}$ (see Table I). Gold was introduced during crystal growth ($[Au_S] < 1 \times 10^{14}\,cm^{-3}$) or after diffusion of an evaporated Au layer at 750 °C in Ar atmosphere for 60 min. Most of the results presented below were performed on samples with gold introduced during the growth. The diffused samples were used for confirmation of the results. Hydrogen was introduced into the samples during wet chemical etching (WCE) in CP4A ($HF:HNO_3:CH_3COOH$ 3:5:3) at room temperature for 2 min. Schottky-contacts were fabricated by resistive evaporation of Au (*n*-type) or Al (*p*-type) through a shadow mask onto the polished side of the sample. Ohmic contacts were made by rubbing a eutectic InGa-alloy onto the backside of the samples. The quality of the Schottky and Ohmic contacts was checked by current-voltage and capacitance-voltage (*C-V*) measurements at room temperature and at 50 K. The *C-V* curves were recorded at 1 MHz. Conventional DLTS and LDLTS were used to investigate the properties of the levels. The intensity of the peaks in the DLTS or LDLTS spectra cannot be directly correlated with the defect concentrations. The concentration depth profiles of the defects were measured by LDLTS with the help of the double pulse technique described in Ref. 18. For the determination of the concentration, the λ-layer was taken into account.[19] The electric field is calculated from *C-V* measurements as described in Ref. 19. Some samples with contacts were subjected to isochronal annealing steps of 30 min in air at different temperatures.

TABLE I. Samples used in the present study.

Samples	Doping (cm^{-3})	Au introduction
n-type FZ-Si (#1)	Phosphorus 3×10^{14}	During crystal growth
n-type FZ-Si (#2)	Phosphorus 1×10^{15}	Diffusion at 750 °C for 60 min.
p-type FZ-Si (#3)	Boron 6×10^{14}	During crystal growth
p-type FZ-Si (#4)	Boron 1×10^{15}	Diffusion at 750 °C for 60 min

III. RESULTS

Figures 1(a) and 1(b) show DLTS spectra from *n*- and *p*-type Au-doped Si after WCE (Samples #1 and #3). Each figure contains two spectra which were recorded at different depths: closer to the surface ($V_R = -2$ V and $V_P = 0$ V) and deeper in the bulk ($V_R = -8$ V and $V_P = -4$ V). The spectra are analogous to those presented in Refs. 11 and 12. The labelling of the DLTS peaks in this work corresponds to that from Ref. 11. In *n*-type Si [Fig. 1(a)], two dominant DLTS peaks were observed at around 105 K and 280 K close to the surface of the samples. By comparing the electrical properties (the activation enthalpy and the capture cross section) of these peaks, we correlate them with G1 at 105 K and with the overlapping levels of $Au_S(-/0)$ and G4 at 280 K. After WCE, the concentration of hydrogen induced centres increased closer to the surface and decreases towards the bulk. In contrast, the concentration of $Au_S(0/+)$ increases towards the bulk of Si. Additional small DLTS peaks are shown close to the surface in Fig. 1(a). However, these peaks were not detected in the Au diffused sample #2 and we will not discuss their origin in this study. In *p*-type Si [Fig. 1(b)], three peaks at 105 K, 160 K, and 205 K were observed. By analysing the electrical properties of these peaks, we assign them to G2 at 105 K, the donor level $Au_S(0/+)$ at 160 K, and G3 at 205 K. The ratio between G2 (G3) and $Au_S(0/+)$ decreases if one measures the defects in the bulk of the hydrogenated *n*-type Si. In the hydrogenated *p*-type Si samples, we also detected two additional DLTS peaks at about 230 K and 270 K. The peak at 270 K might be related to the Au acceptor level $Au_S(-/0)$. However, both peaks were not observed in the Au diffused sample #4. Therefore, in the following, we will not discuss their origin. All DLTS peaks labelled in Figs. 1(a) and 1(b) were also detected in the Au diffused samples (#2 and #4) after WCE.

Figures 2(a) and 2(b) present the LDLTS spectra of the dominant DLTS peaks in the *n*- and *p*-type Si samples #1 and #3. These spectra are plotted on the same emission rate

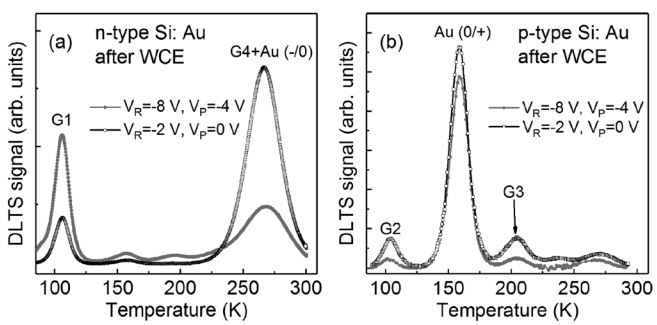

FIG. 1. DLTS spectra recorded from samples #1 (a) and #3 (b) after WCE. The spectra are recorded with different filling pulses and monitor the levels close to the surface and in the bulk.

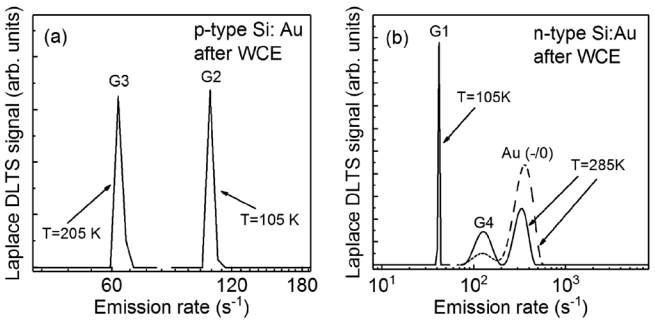

FIG. 2. Laplace DLTS spectra recorded from sample #1 in *n*-type (a) and from sample #3 in *p*-type *p*-type (b) at different temperatures after WCE. The solid and dashed lines show the spectra recorded close to the surface and in the bulk of the samples, respectively.

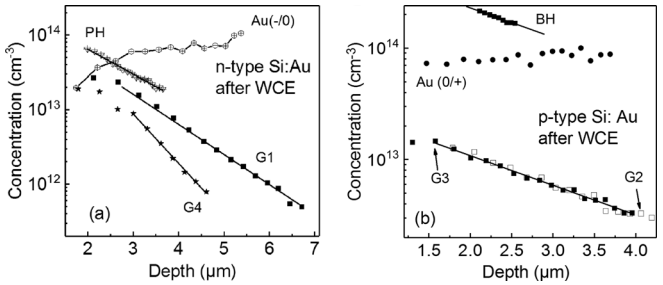

FIG. 3. Concentration depth profiles of G1-G4, $Au_S(-/0)$, $Au_S(0/+)$, boron-hydrogen, and phosphorous-hydrogen complexes recorded after WCE in sample #1 (*n*-type Si) and sample #3 (*p*-type Si). The solid lines are fits to the defect concentrations in the bulk of Si.

axis for *p*-type and *n*-type Si, but they were recorded at different temperatures. The solid line shows the spectra which were recorded close to the surface and the broken line in Fig. 2(b) exhibits the spectrum recorded deeper in the bulk. Single Laplace DLTS peaks were observed for G1, G2, and G3. In good agreement with the results of Ref. 14, the intensities of G4 and $Au_S(-/0)$ are comparable in the region with more hydrogen (close to the surface) and $Au_S(-/0)$ is dominant deeper in the bulk where the H content is reduced. One should emphasize that the width of the LDLTS peaks recorded at 285 K in *n*-type Si is larger in comparison to that observed in the spectra at lower temperatures. This can be explained by the higher temperature of the measurements which reduces the resolution of the LDLTS technique.

Similar LDLTS spectra were recorded in the Au diffused *n*- and *p*-type Si samples #2 and #4. The activation enthalpies of the G1-G4 defects were obtained from the Arrhenius plots. The apparent capture cross sections σ_a were determined from the extrapolation of the Arrhenius plots towards high temperatures. All values are given in Table II.

The concentration depth profiles of the G1-G4 levels were determined in the WCE samples by the double pulse LDLTS technique. Figures 3(a) and 3(b) compare the depth profiles of G1-G4, the Au donor and acceptor levels, and the profiles of the passive phosphorous-hydrogen (PH) and boron-hydrogen (BH) complexes. The PH and BH profiles were obtained by subtraction of the net free carrier concentration in the hydrogenated sample from the original free carrier concentration before hydrogenation. The solid lines in Fig. 3 describe linear fits to the data points (excluded are points close to the surface). The depth profiles of G1-G4 are descending towards the bulk of Si. The profiles of G1 and G4 are not identical. This behaviour contradicts the assumed model that both levels belong to the same defect.[10–12,14] The slope of the concentration profile of G1 is identical to that observed for the PH complex, whereas the slope of the concentration profile of G4 is a factor of ~1.7 steeper.

TABLE II. Electrical properties of Au and AuH-related defects observed in this study. The activation enthalpy and the apparent capture cross section σ_a were determined by LDLTS from the Arrhenius plot [ln (emission rate/T^2 vs 1/T)]. The theory values for the enthalpies are presented for the respective Au complexes. Due to our new assignments, the correlation of the levels with the G-labeling used in Ref. 40 was changed. Directly measured capture cross sections σ are listed from the literature.

Labelling of energy levels	Activation enthalpy (a) exp. this work, (b) exp. (Ref.), and (c) theory (Ref.) (eV)	Apparent capture cross section (this work) (cm^2)	Capture cross section from the literature (cm^2)	Level identification
Au (−/0)	(a) $E_C - 0.56$	3×10^{-15}	1×10^{-16} (Refs. 11 and 14)	Au (−/0)
	(b) $E_C - 0.558$[14]			
	(c) $E_C - 0.66$[40]			
Au (0/+)	(a) $E_V + 0.34$	5×10^{-14}	3×10^{-15} (Ref. 12)	Au (0/+)
	(b) $E_V + 0.33$[31]		1×10^{-15} (Ref. 11)	
	(c) $E_V + 0.21$[40]			
G1	(a) $E_C - 0.19$	5×10^{-16}	1×10^{-17} (Ref. 11)	AuH_1 (2−/−)
	(b) $E_C - 0.19$[11]			
	(c) $E_C - 0.22$[40]			
G3	(a) $E_V + 0.43$	2×10^{-14}	9×10^{-15} (Ref. 12)	AuH_1 (−/0)
	(b) $E_V + 0.47$[11]		5×10^{-16} (Ref. 11)	
	(c) $Ev + 0.62$[40]			
G2	(a) $E_V + 0.17$	4×10^{-16}	4×10^{-15} (Ref. 12)	AuH_1 (0/+)
	(b) $E_V + 0.21$[11]		2×10^{-15} (Ref. 11)	
	(c) $E_V + 0.36$[40]			
G4	(a) $E_C - 0.53$	5×10^{-16}	6×10^{-17} (Ref. 14)	AuH_2 (−/0)
	(b) $E_C - 0.542$[14]			
	(c) $E_C - 0.62$[40]			

In Fig. 3(b), the depth profiles of G2 and G3 are identical and the slopes are comparable to that of BH. In contrast to G1-G4, the concentration of $Au_S(-/0)$ and $Au_S(0/+)$ increases towards the bulk of Si and the minimum of the concentration of this defect is observed close to the surface of Si. The reduced concentration of Au_S at the surface agrees with the formation of AuH complexes.

The majority carrier emission rates for G1, G2, and G3 were investigated by applying different electrical fields to the Schottky diode (Fig. 4). We used the double pulse LDLTS technique with two fixed filling pulses to probe the defects at the same depth in the depletion region, whereas the electrical field was varied by the applied reverse bias. No changes in the emission rate of G3 were observed in the investigated range of the electrical field. In contrast, the emission rates of G1 and G2 increase linearly with the square of the electric field. However, this increase is significantly smaller compared to the Poole Frenkel effect, which describes a carrier emission from a Coulombic centre. Due to the close electrical properties (activation enthalpy and apparent capture cross section) of G4 and $Au_S(-/0)$, we were not able to measure the field dependence of G4 properly.

Annealing of G2 and G3 above room temperature reduces their concentrations. Figure 5 gives the concentrations after 30 min isochronal annealing steps at different temperatures. The measurements of the concentration were always performed at a depth of about 1.6–2.1 μm. We found that G2 and G3 annealed at an identical temperature of about 370 K. With the decrease in the G2 concentration, a new LDLTS line G2′ grows in (Fig. 6). The electrical properties of G2′ are close to those of G2 and these two defects cannot be reliably resolved in the conventional DLTS spectra.

IV. DISCUSSION

Our results confirm that G1, G2, G3, and G4 are induced by hydrogen in Au doped Si. The levels form at the expense of the Au_S concentration and belong to defects with hydrogen bound to substitutional Au. The presence of the AuH defects does not depend on the method of Au introduction into Si.

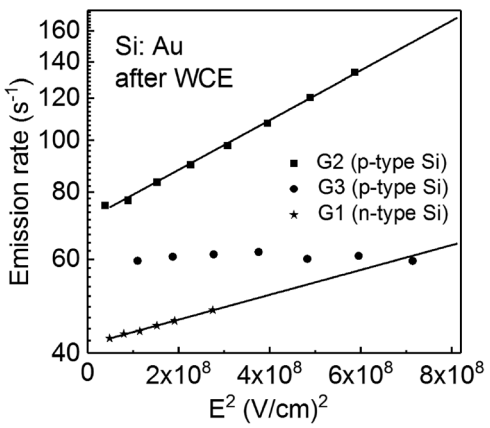

FIG. 4. Emission rate versus the square of the electric field for G1-G3 recorded in samples #1 and #3. The solid lines show linear fits to the experimental data.

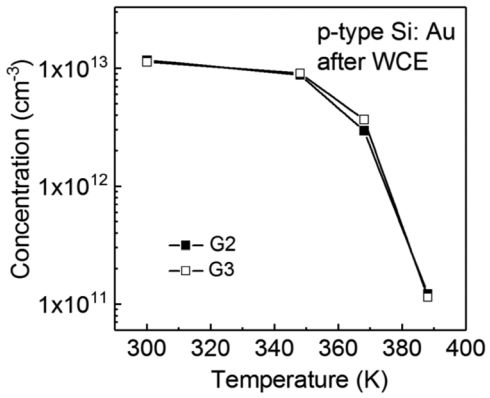

FIG. 5. Concentrations of G2 and G3 in sample #3 as a function of isochronal annealing (30 min). The measurements were performed at about 1.6–2.1 μm from the surface of Si.

In contrast to previous studies, we cannot attribute G1, G2, and G4 to different charge states of the same AuH complex. The concentrations of G1 and G4 in *n*-type Si are within a factor of 1.5–2 close to the surface and differ significantly in the bulk. Under our experimental conditions of a low temperature hydrogen in-diffusion and a homogeneous substitutional Au concentration in the melt doped samples, a simple successive binding of hydrogen atoms to substitutional Au is proposed. Feklisova and Yarykin demonstrated that the depth profiles of H-related defect concentrations after WCE were related to the number of H atoms in the corresponding defects.[20] Identical slopes for PH and G1 suggest that similar to PH the G1 defect should contain one single H atom. A comparison of the slopes of the G1 and G4 profiles gives a difference of a factor of ∼1.7. Therefore, we assign G1 to the AuH_1 and G4 to the AuH_2 defect. The contradicting results presented in Ref. 11 can be explained by the analysis of the overlapping G1 and G4. As shown in Fig. 3, the concentration of $Au_S(-/0)$ is not negligible in comparison to G4 close to the surface and, therefore, the determination of the concentration of G4 cannot be directly obtained from conventional DLTS measurements under the assumptions made in Ref. 11. No depth profiles of G1 and G4 were

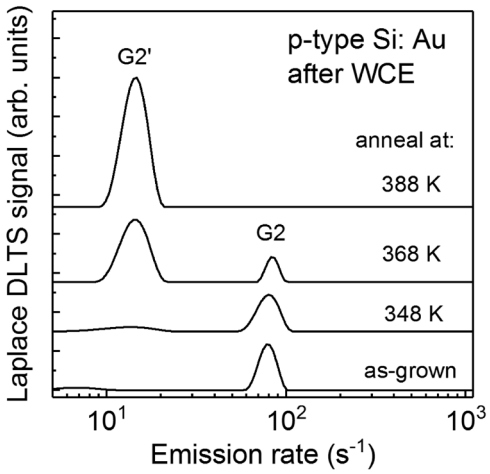

FIG. 6. Representative LDLTS spectra recorded at 105 K after the 30 min isochronal annealing steps from Fig. 5.

presented in Ref. 14, which is the only study where both levels were measured separately.

In our *p*-type Si samples, the depth profiles of G2 and G3 were found to be always identical. The slope of the concentration reduction matches that of the passive BH-complexes and this suggests that G2 and G3 are different charge states of the same AuH_1 complex with only one hydrogen atom. This assignment is further supported by the identical annealing behavior of both levels (see Fig. 5). In Ref. 11, the annealing behavior of G2 and G3 was found to be different (G2 was more stable in comparison to G3). This difference could be explained by the LDLTS spectra shown Fig. 6. After annealing at about 350 K, another LDLTS peak labelled G2′ was observed. This peak becomes dominant after annealing at higher temperatures. It is out of the scope of this study to shed light on the origin of this defect. This might be another Au-related defect since we did not observe this peak in other samples without Au. By using the conventional DLTS technique, G2′ could not be resolved from G2 and this might have led to the erroneous conclusions in Ref. 11 that the annealing temperature of G2 and G3 was different.

The sum of the concentrations of G1, G4, and $Au_S(-/0)$ close to the surface in Fig. 3(a) is smaller in comparison to the total concentration of $Au_S(-/0)$ in the bulk. By assuming that gold interacts only with hydrogen in our samples, a passive AuH_x defect seems likely to be present in this region. Similar passive defects were also reported in Refs. 8 and 9. However, their hydrogen concentrations were significantly higher in comparison to those observed in our samples, due to the different procedures of H introduction.

Information on the charge states of defects is usually indirectly inferred from capture cross sections and the dependence of emission rates on the electrical field. The emission of a carrier from a binding Coulomb potential in an electric field was first proposed and calculated by Frenkel.[21] In this case, the logarithm of the emission rates shows a typical square root dependence on the electric field. Such an enhancement of the emission rate of a defect is a good indication of its donor-/acceptor-like behavior in the upper/lower half of the band gap.[22] However, the effect of an electric field on the emission rate of defects which are supposed to

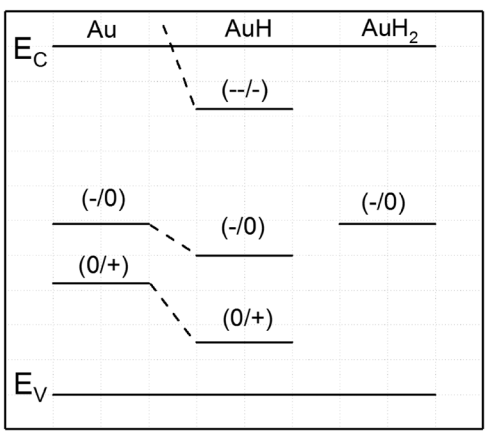

FIG. 7. Schematic diagram of Au and AuH-related levels in the band gap of hydrogenated Si.

be donors in *n*-type or acceptors in *p*-type semiconductors is often much smaller than that expected by the Frenkel theory. Therefore, strong efforts were undertaken to describe the enhancement of the emission rates under electric field for different non-Coulombic model potentials of deep defects. An overview is given in Ref. 23, which also includes the important contribution of phonon-assisted tunneling in the emission process.[24,25] The main outcome of these studies is that one cannot always straightforwardly deduce the charge state of the defect from the electric field dependence of its emission rate. A direct and simple evaluation of the defect charge state is only possible for Coulombic centers which exhibit the Poole-Frenkel effect for small electric fields. At larger fields, phonon assisted tunneling or direct tunneling becomes dominant.[26,27] Karpus and Perel[28] derived a critical electric field strength, which should distinguish between the Poole Frenkel effect and the phonon assisted tunneling mechanism. For Si, this critical field can be estimated to be smaller than $\sim 10^3$ V/cm. Electric field dependent emission rates from carbon-hydrogen defects support the existence of a critical field at slightly higher values (2×10^4 V/cm).[29]

For the electron capture at the Au acceptor, a temperature independent capture cross section of $\sim 1 \times 10^{-16}$ cm^2 was reported. The electron emission rate showed a weak dependence on the electric field above $\sim 2 \times 10^4$ V/cm.[30] The same behaviour was found for the hole emission from the Au donor level. A temperature independent capture cross section of $\sim 3 \times 10^{-15}$ cm^2 and no field dependence of the hole emission up to 10^5 V/cm were detected.[2,31,32]

In Table II and Fig. 7, we give a summary of the properties of all measured levels in this study. Our results of the activation enthalpies are compared to experimental and theoretical results of other authors. The differences of the referenced experimental data with our values should be taken as indication of the error bar for these level positions. Based on our LDLTS measurements, activation enthalpy and apparent carrier capture cross section σ_a were derived from the Arrhenius plots of the logarithm of the T^2 corrected emission rates versus 1/T. We also list typical, directly determined capture cross sections σ from filling pulse measurements from the literature. Our level assignment is based essentially on the magnitude of σ. The values for substitutional Au are in agreement with the calculation by Lax for a non-Coulombic binding centre and can be related to the acceptor $Au_S(-/0)$ or donor $Au_S(0/+)$ state.[33] The capture cross section of G2 is comparable to $Au_S(0/+)$ and we assign this level in agreement with Ref. 11 to the donor state of AuH_1. Attractive Coulomb potentials should give rise to an increased σ. However, the differences calculated by Tasch and Sah in the polarisation model of Lax for the minority carrier emission of the Au acceptor do not differ significantly from the majority carrier cross sections.[2] We correlate therefore G3, which has the same depth profile and identical annealing properties as G2 with the acceptor state of AuH_1. G1 belongs to the same AuH_1 complex and the small value of σ is typical for a capture into a repulsive centre AuH_1 (2−/−). The repulsive potential was directly verified by temperature dependent capture cross section measurements, which gave a repulsive barrier of 21 ± 2 meV.[34] The small

value of σ for G4, the only level detected from the AuH_2 complex, could relate this centre to the double acceptor of AuH_2. However, we will give arguments below for another level assignment.

A comparison of σ with σ_a in Table II gives further support for our level identification. Usually, σ_a is larger than σ. The difference is generally attributed to an entropy factor, which accounts for electronic and vibronic changes during the emission of the carriers (for details see Ref. 3). Large entropy changes after the majority carrier emission were reported for the Au donor and acceptor states in Refs. 35 and 36. According to Watkins and Williams[37] and Van Vechten and Thurmond,[38] the electronic and structural properties of substitutional Au can be visualised by the occupation of the dangling bond states of an ideal vacancy. In this model, the electrical properties of neutral Au_S are described by the singly negatively charged vacancy V^-. The binding of a neutral hydrogen atom to Au_S will introduce one extra electron into the vacancy. The properties of the neutral AuH_1 complex correspond therefore to the configuration V^{2-}.

An analogous model was introduced to explain successfully the properties of vacancy hydrogen complexes in Si.[39] Emission of an electron from a stable vacancy structure with even number of electrons (saturated bonds) leads to a strong reconfiguration during charge emission.[38] The reconfiguration could explain the entropy increase observed after electron emission from the $AuH_1(2-)$ state (G1) and hole emission from the $AuH_1(0)$ state (G3). In Table II, only G2 shows a smaller σ_a compared to σ. This is in agreement with the above argument. G2 describes the hole emission from the positive $AuH_1(+)$ state, which corresponds to V^- with an odd number of electrons. A large entropy change is not expected for this transition and the reduction of σ_a could be related to spin degeneracies of the involved states.

The entropy changes of the electron emission from the G4 level are in agreement with AuH_2 (−/0), which corresponds to an emission from the vacancy level with even number of electrons. The alternative assignment of AuH_2 to the (2−/−) state has to be discarded, due to calculations reported in Ref. 40.

The electric field enhancement of the emission rates of G1 and G2 shows a quadratic dependence on the electric field (Fig. 4). The shift is however much smaller as expected for an emission from a coulomb center (Poole Frenkel effect). According to the discussion given above for Au_S, this field dependence is expected if the emission is dominated by multi-phonon participation.[26,27] No information about the charge state of the defects can be derived in this field range. Lower electric fields could be achieved in the lower doped material. However, the lower doping also leads to a shift of the probed depletion region towards the bulk (around 10 μm for the samples with a doping level of about $10^{14}\,cm^{-3}$). This makes it difficult to detect H-related defects located in the vicinity of the surface (generally up to 2–5 μm) in these samples by the LDLTS technique. The G3 line, which corresponds according to our assignment to a hole emission from a Coulombic center, shows no electric field dependence in the investigated range. Buchwald and Johnson showed that the Poole-Frenkel effect could be significantly suppressed for a defect with the attractive Coulombic potential due to the presence of the barrier for the capture of electrons (holes).[41] Sveinbjörnson has detected, however, no barrier for carrier capture and, therefore, the explanation of the field dependence is still open.[11] The analysis of the electric field dependence needs further experimental and theoretical consideration. State of the art calculations of the capture cross section like those in Ref. 42 with the inclusion of an applied electric field could give detailed information about the defect potential and the lattice coupling.

Our level assignment for G1 and G3 agrees with the estimated level positions for the AuH_1 complex, which were derived from the properties of the AuH local mode spectra.[16] The results presented in this study are also consistent with those from calculations (see Table II) in Refs. 40 and 44. One should also emphasize that the acceptor states of AuH_3 and AuH_4 were predicted to be electrically active in Si in Refs. 43 and 44. However, no traces of these complexes were observed in hydrogenated Si by wet chemical etching in the present study.

Rubaldo *et al.*[45] reported the presence of another level G4′ with an activation enthalpy of about 580 meV below the conduction band. This defect was tentatively correlated with the acceptor state of AuH_3. However, we have never observed this level in our samples. From the reported activation enthalpy, we cannot rule out that G4′ is related to a level of a CH defect.[46]

V. SUMMARY

Hydrogen was introduced by wet chemical etching at room temperature into *n*-type and *p*-type Si doped with Au. Four dominant levels G1-G4 were detected in these samples and investigated by LDLTS. From the depth profiles of the levels, we conclude that G1 and G4 belong to two different AuH defects with one (AuH_1) and two (AuH_2) H atoms, respectively. G2 and G3 were shown to belong to different charge states of the same AuH_1 defect. By analyzing the reported values of the majority carrier capture coefficients σ and comparing them with the values of the apparent capture cross sections σ_a evidence for the charge state of the levels is derived. We attribute G1 to the double acceptor state of $AuH_1(2-/-)$, G3 to the single acceptor state $AuH_1(-/0)$, and G2 to the single donor state $AuH_1(0/+)$. The G4 line is tentatively correlated with the single acceptor state of the Au center with two hydrogen atoms (AuH_2).

ACKNOWLEDGMENTS

The authors thank Dr. Abrosimov and Dr. Lemke for supplying the samples with gold introduced during the growth. K.G. acknowledges the scholarship from the special-purpose grant awarded to Faculty of Fundamental Problems of Technology at Wroclaw University of Science and Technology by Ministry of Science and Higher Education in 2017 for research and development of the young scientists and Ph.D. students and statutory Grant No. 0401/0009/17.

[1]C. B. Collins, R. O. Carlson, and C. J. Gallagher, Phys. Rev. **105**, 1168 (1957).
[2]A. F. Tasch and C. T. Sah, Phys. Rev. B **1**, 800 (1970).
[3]V. Lang, H. G. Grimmeiss, E. Meijer, and M. Jaros, Phys. Rev. B **22**, 3917 (1980).
[4]L.-Å. Lebedo and Z. G. Wang, Appl. Phys. Lett. **42**, 680 (1983).
[5]J. Utzig and W. Schröter, Appl. Phys. Lett. **45**, 761 (1984).
[6]J. W. Petersen and J. Nielsen, Appl. Phys. Lett. **56**, 1122 (1990).
[7]G. D. Watkins, M. Kleverman, A. Thilderkvist, and H. G. Grimmeiss, Phys. Rev. Lett. **67**, 1149 (1991).
[8]S. J. Pearton and A. J. Tavendale, Phys. Rev. B **26**, 7105 (1982).
[9]S. J. Pearton, W. L. Hansen, E. E. Haller, and J. M. Kahn, J. Appl. Phys. **55**, 1221 (1984).
[10]E. Ö. Sveinjbörnsson and O. Engström, Appl. Phys. Lett. **61**, 2323 (1992).
[11]E. Ö. Sveinjbörnsson and O. Engström, Phys. Rev. B **52**, 4884 (1995).
[12]J. A. Davidson and J. H. Evans, Semicond. Sci. Technol. **11**, 1704 (1996).
[13]A. Zamouche, J. Appl. Phys. **93**, 753 (2003).
[14]P. Deixler, J. Terry, I. D. Hawkins, J. H. Evans-Freeman, A. R. Peaker, L. Rubaldo, D. K. Maude, J.-C. Portal, L. Dobaczewski, K. B. Nielsen, A. Nylandsted Larsen, and A. Mesli, Appl. Phys. Lett. **73**, 3126 (1998).
[15]A. L. Parakhonskii, O. V. Feklisova, S. S. Karelin, and N. Yarykin, Semiconductors **30**, 362 (1996).
[16]M. J. Evans, M. Stavola, M. G. Weinstein, and S. J. Uftring, Mater. Sci. Eng. B **58**, 118 (1999).
[17]P. T. Huy and C. A. J. Ammerlaan, Physica B **302–303**, 233 (2001).
[18]L. Dobaczewski, A. R. Peaker, and K. Bonde Nielsen, J. Appl. Phys. **96**, 4689 (2004).
[19]P. Blood and P. W. Orton, *The Electrical Characterization of Semiconductors: Majority Carriers and Electron States* (Academic Press, 1992).
[20]O. Feklisova and N. Yarykin, Semicond. Sci. Technol. **12**, 742 (1997).
[21]J. Frenkel, Phys. Rev. **54**, 647 (1938).
[22]J. L. Hartke, J. Appl. Phys. **39**, 4871 (1968).
[23]P. A. Martin, B. G. Streetman, and K. Hess, J. Appl. Phys. **52**, 7409 (1981).
[24]S. Makram-Ebeid and M. Lannoo, Phys. Rev. B **25**, 6406 (1982).
[25]V. Karpus and V. I. Perel, JETP Lett. **64**, 1376 (1986).
[26]G. Vincent, A. Chantre, and D. Bois, J. Appl. Phys. **50**, 5484 (1979).
[27]S. D. Ganichev, E. Ziemann, W. Prettl, I. N. Yassievich, A. A. Istratov, and E. R. Weber, Phys. Rev B **61**, 10361 (2000).
[28]V. Karpus and V. I. Perel, JETP Lett. **42**, 498 (1985).
[29]R. Stübner, Vl. Kolkovsky, and J. Weber, J. Appl. Phys. **118**, 055704 (2015).
[30]L. S. Lu and C. T. Sah, J. Appl. Phys. **59**, 173 (1986).
[31]L. S. Lu, T. Nishida, and C.-T. Sah, J. Appl. Phys. **62**, 4773 (1987).
[32]A. Mesli, E. Courcelle, T. Zundel, and P. Siffert, Phys. Rev B **36**, 8049 (1987).
[33]M. Lax, Phys. Rev. **119**, 1502 (1960).
[34]J. U. Sachse, PhD thesis, MPI_Stuttgart, 1997.
[35]I. Dudeck and R. Kassing, Phys. Status Solidi A **49**, 153 (1978).
[36]R. Kassing, L. Cohausz, P. van Staa, W. Mackert, and H. J. Hoffman, Appl. Phys. A **34**, 41 (1984).
[37]G. D. Watkins and P. M. Williams, Phys. Rev. B **52**, 16575 (1995).
[38]J. A. VanVechten and C. D. Thurmond, Phys. Rev. B **14**, 3539 (1976).
[39]B. Bech Nielsen, P. Johannesen, P. Stallinga, K. Bonde Nielsen, and J. R. Byberg, Phys. Rev. Lett. **79**, 1507 (1997).
[40]A. Resende, R. Jones, S. Öberg, and P. R. Briddon, Phys. Rev. Lett. **82**, 2111 (1999).
[41]W. R. Buchwald and N. M. Johnson, J. Appl. Phys. **64**, 958 (1988).
[42]A. Alkauskas, Q. Yan, and C. G. Van de Walle, Phys. Rev. B **90**, 075202 (2014).
[43]A. Resende, J. Goss, P. R. Briddon, S. Öberg, and R. Jones, Mater. Sci. Forum **258–263**, 295 (1997).
[44]R. Jones, B. J. Coomer, J. P. Goss, B. Hourahine, and A. Resende, Solid State Phenom. **71**, 173 (2000).
[45]L. Rubaldo, P. Deixler, I. D. Hawkins, J. Terry, D. K. Maude, J.-C. Portal, J. H. Evans-Freeman, L. Dobaczewski, and A. R. Peaker, Mater. Sci. Eng., B **58**, 126 (1999).
[46]R. Stübner, L. Scheffler, Vl. Kolkovsky, and J. Weber, J. Appl. Phys. **119**, 205709 (2016).